The approximate use of 1D internal multiple prediction in a multidimensional world: errors and recommendations

Pan Pan, CREWES, University of Calgary, Calgary, Alberta, Canada, panp@ucalgary.ca*
Kris Innanen, CREWES, University of Calgary, Calgary, Alberta, Canada, k.innanen@ucalgary.ca

Summary

In this paper, we numerically analyze a 1D version of the internal multiple prediction algorithm developed by Weglein and collaborators in the 1990s. Multiples generated by dipping and diffractive structures, and multiples measured at significant offset are not handled by the 1D algorithm, and in principle require the use of 1.5D, 2D and/or 3D versions. But in practice errors from dip and offset accrue gradually. To maximize the usefulness of the 1D algorithm, which is very fast, we analyze with synthetic data the rate at which these errors compound. We review the basic form of the internal multiple prediction algorithm, and then begin examining its performance on synthetic data sets. We systematically study how the presence of offset and the existence of dipping angle in the reflectors affect the 1D internal multiple prediction algorithm. The results allow us to make some broad recommendations for the application of this method given estimated ranges of dips of potential multiple generators, and ratios of offset to generator depths.

Introduction

For the exploration of oil and gas reservoirs, multiples can be one of the main challenges faced by seismic methods. According to the classification of Xiao et al. (2003), there are three basic methods for suppressing multiples. The first type is deconvolution methods, which use the periodicity of multiples for suppression and are effective in suppressing short period free surface multiples generated at shallow reflectors. Secondly, filtering methods use differential moveout between primaries and multiples that are separated in the f-k,τ-p, or Radon domains. These filtering methods can successfully suppress multiples generated at moderate to deep reflectors where multiples are well-separated from their primaries. However, the above two methods assume that the earth is one dimensional with horizontal uniform layers. Dipping reflectors and variations in the overburden can cause serious problem in those methods. However, the third type of methods, wavefield prediction and subtraction, overcome these problems. These methods are based on the wave equation and use recorded data to predict multiples by wave extrapolation and inversion procedures. These wavefield methods obtain multiple-free data by subtracting the predicted multiples and can suppress all multiples generated by any complex system of reflectors.

The internal multiple prediction method that we use in this paper is derived from inverse scattering series, which belongs to wavefield methods. This method is capable of attenuating internal multiples in 1D, 2D and 3D without any a priori information about the medium. It can be applied to zero offset data without assuming multiple periodicity.

Internal multiple prediction

For detailed development of the inverse scattering series and its use in deriving the internal multiples attenuation please see Weglein et al. (1997; 2003). Here we will confine ourselves to study of the prediction algorithm in 1D, assuming zero offset data, in which case the algorithm is

$$b_{3IM}(k_z) = \int_{-\infty}^{\infty} dz e^{ik_z z} b_1(z) \int_{-\infty}^{z-\epsilon} dz' e^{-ik_z z'} b_1(z') \int_{z'+\epsilon}^{\infty} dz'' e^{ik_z z''} b_1(z''), \quad (1)$$

$k_z = 2\omega/c_0$ is the vertical wavenumber, which is the conjugate of the pseudo-depth ($z = c_0 t/2$), c_0 is the constant reference velocity, $b_{3IM}(k_z)$ is the prediction of the internal multiples. The $b_1(z)$ entries are the input data traces in pseudo-depth.

The above algorithm is composed of three events that satisfy $z'' > z'$ and $z > z'$. The travel time of the internal multiple is the sum of the travel times of the two lower events which are $b_1(z)$ and $b_1(z'')$, minus the travel time of the higher event, $b_1(z')$. The parameter ϵ is included in equation 1 to ensure that $z'' > z'$ and $z > z'$. For band-limited data, this parameter is related to the width of the wavelet.

The inverse scattering series based internal multiple prediction method (Araújo et al., 1994; Weglein et al., 1997) is fully data-driven. Any information about the reflectors that generate the internal multiples or the medium through which the multiples propagate is not required (Luo et al., 2011). It predicts all the internal multiples from all possible generators at once. It also predicts the correct travel times and approximate amplitudes of all the internal multiples which is demonstrated using the subevent interpretation (Weglein and Matson, 1998). Hernandez et al. (2011, 2012) have studied land and physical modeling applications of 1D prediction. In this paper, we continue to study the 1D algorithm.

Systematic study of prediction errors

In this part, we will systematically study the prediction errors. First of all, we build a velocity model with horizontal interfaces, and calculate a shot record. The velocity model is shown in Figure 1 (a) and the shot record is shown in Figure 1 (b). The direct wave is removed. Acoustic finite difference forward modeling codes developed at CREWES (*www.crewes.org*) are used to create the data. To avoid free surface multiples, we need to ensure that the boundary condition is absorbing on all four sides. The data were generated with lowcut, lowpass, highpass and highcut frequencies of 10Hz, 20Hz, 80Hz and 100Hz respectively. All the remaining parameters are listed in Table 1.

We select traces from this shot record to be input into the internal multiple prediction algorithm. The 1D internal multiple algorithm is expected to accurately predict multiple arrival times at zero offset trace (in the center of the shot record). Several tests are made with this benchmark trace to choose the optimum epsilon value. This was determined to 60 sample points, using the fact that artifacts from badly chosen epsilon values will often arise at the arrival times of the primaries in the output. In Figure 3 the result of applying the prediction code is illustrated, with the input zero offset trace in Figure 3 (a), and the prediction in Figure 3 (b). We focus on the two major internal multiples with arrival times are t_1=0.67s and t_2=0.97s. In Figures 3 (a)-(b), the red circles indicate the positions of the internal multiples in the input and output data. With this benchmark test in place and an optimum epsilon value determined, we are ready to proceed with the offset tests.

The influence of the offset

We will measure the prediction errors produced in the prediction of internal multiples 1 and 2, respectively, as we increase the offset of the input traces.

Through manual picking the relative travel time error between predicted and actual multiples is plotted in Figure 4. We can see that as the offset becomes larger, prediction error increases. When the offset reaches 360 m, which is 180% of the depth of the generator, the prediction result rises above 8% for the first internal multiple and 6% for the second one. We see this as a qualitative threshold below which the error level is likely accept.

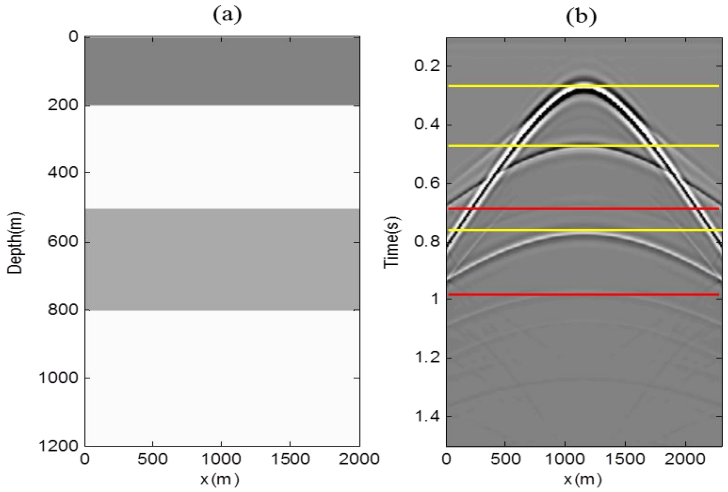

Figure 1: (a) Four-layer velocity model. (b) Shot record with primaries and internal multiples shown. Yellow lines indicate the positions of primaries, and red lines indicate the positions of internal multiples.

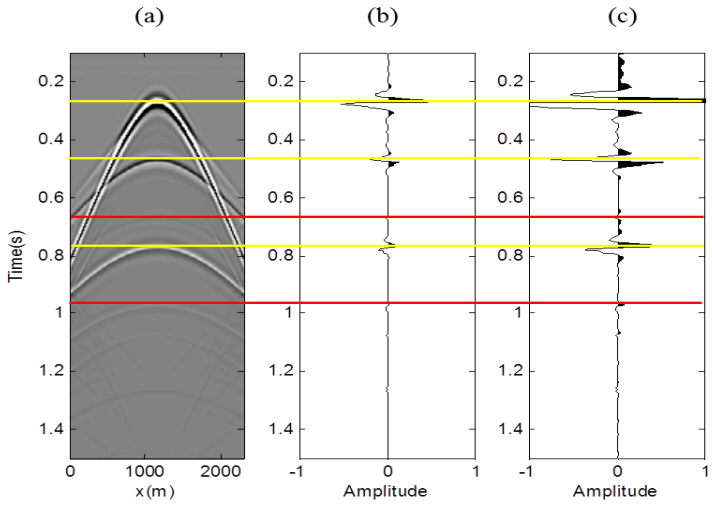

Figure 2: (a) Shot record of the model. (b) Zero offset trace plotted in wiggle format with a scale of 5. (c) The same trace as (b) with a larger scale of 20. Yellow lines indicate the locations of primaries, and red lines indicate the locations of internal multiples.

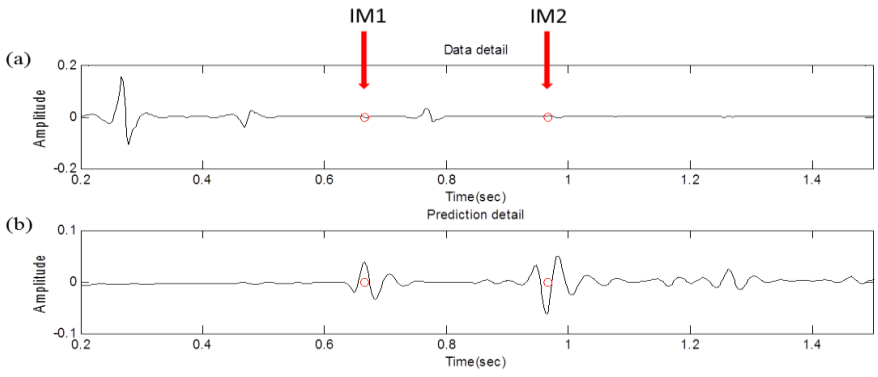

Figure 3: Application of the internal multiple prediction algorithm to the zero offset trace. (a) Input data. (b) Prediction output. The red circles indicate the positions of the internal multiples in the input and output data.

Table 1: Parameters of the velocity model and shot record

PARAMETER	VALUE
Number of t	1024
Number of x	1024
Number of z	1024
Interval sample time	3ms
Velocity and depth of the first interface	3000m/s at 200m
Velocity and depth of the second interface	2000m/s at 500m
Velocity and depth of the third interface	3000m/s at 800m
Wave speed of the source/ receiver medium	1500m/s
Time step	0.4ms
Maximum time of the shot record	3.07s
Location of the source	(1, 512)
Frequency band (Hz)	[10 20 80 100]
Epsilon	60

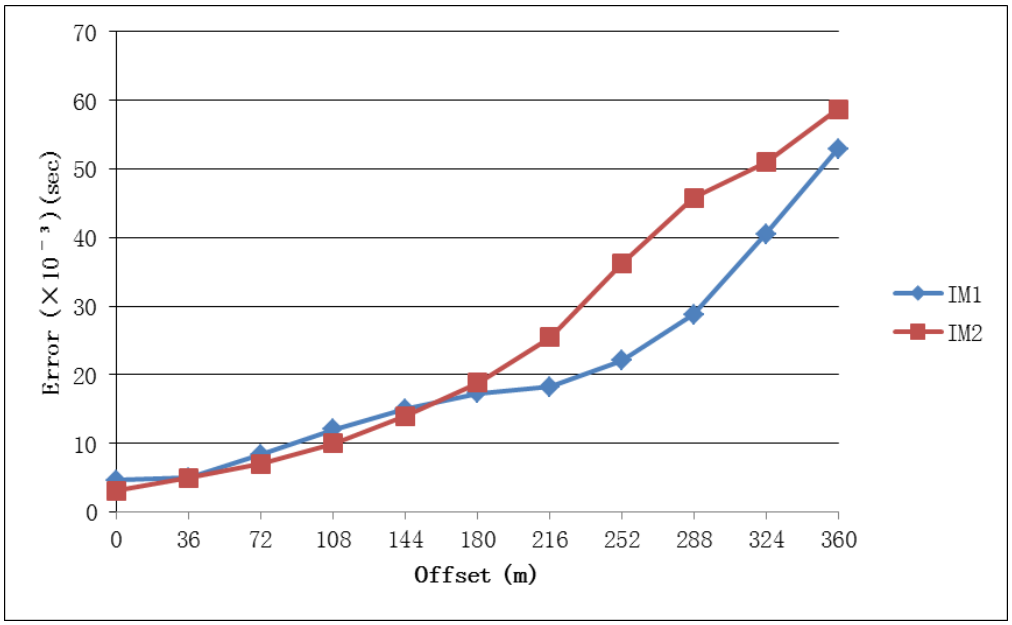

Figure 4: Prediction errors plotted against an increasing series of offset

The influence of the dipping angle

Next we analyze the prediction error in the zero offset trace over dipping interfaces, allowing the dip angles to gradually increase from 0 to 15 degrees. The three cases examined are

(1) where the first interface (i.e., the generator) is the dipping interface, (2) where the second interface is the dipping interface, and (3) where the third interface is the dipping interface.

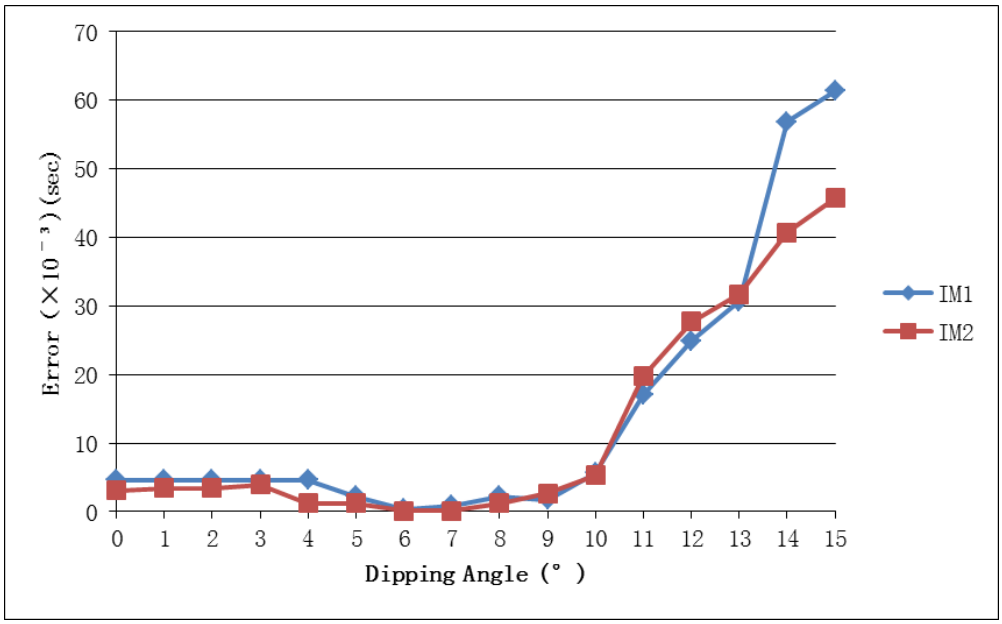

Figure 5: Prediction errors in the zero offset trace plotted against an increasing series of dipping angles, the generator is the dipping interface.

First, we will study what happens when the generator is the dipping interface. In Figure 5, the blue line is the prediction error of the internal multiple 1 and the red line is the prediction error of the internal multiple 2. The graph shows that all errors are within 1% in the range of 0-10 degrees, with a sharp increase starting after 10 degrees. This means that when the first interface is the dipping interface, the algorithm will yield acceptable results in the range of 0-10 degrees.

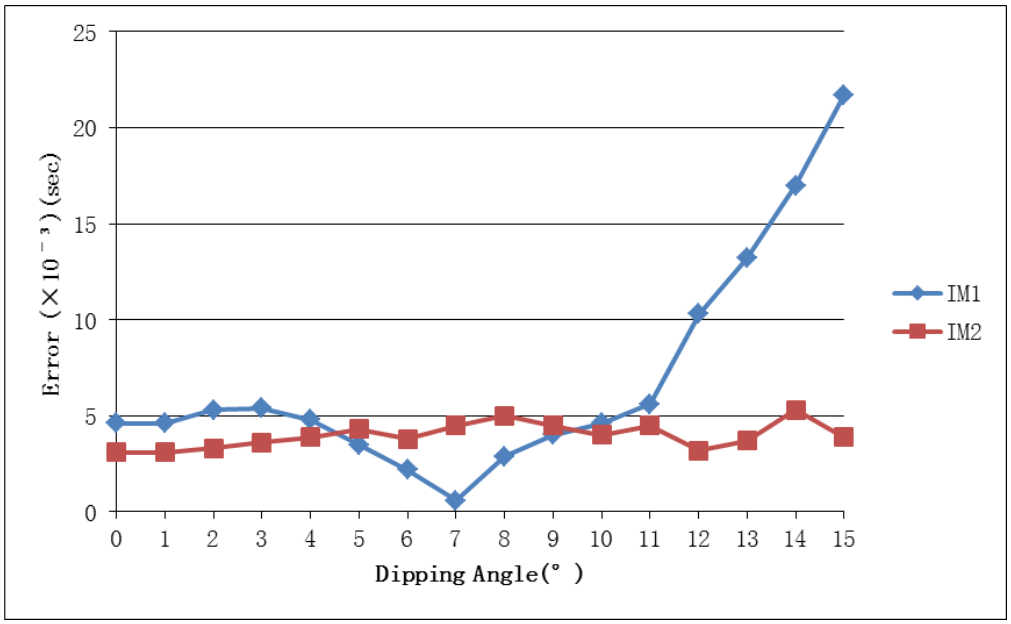

Figure 6: Prediction error in the zero offset trace plotted against an increasing series of dipping angles, the second interface is the dipping interface.

We next analyze the effect of the second interface becoming the dipping interface. In Figure 6, the graph displays larger fluctuations in the first internal multiple than the second one, implying a greater effect on the first internal multiple. Error of internal multiple 1 is within 1% for the range of 0-11 degrees, and increases sharply thereafter. Errors of internal multiple 2 remain within 1% for the range of 0-15 degrees.

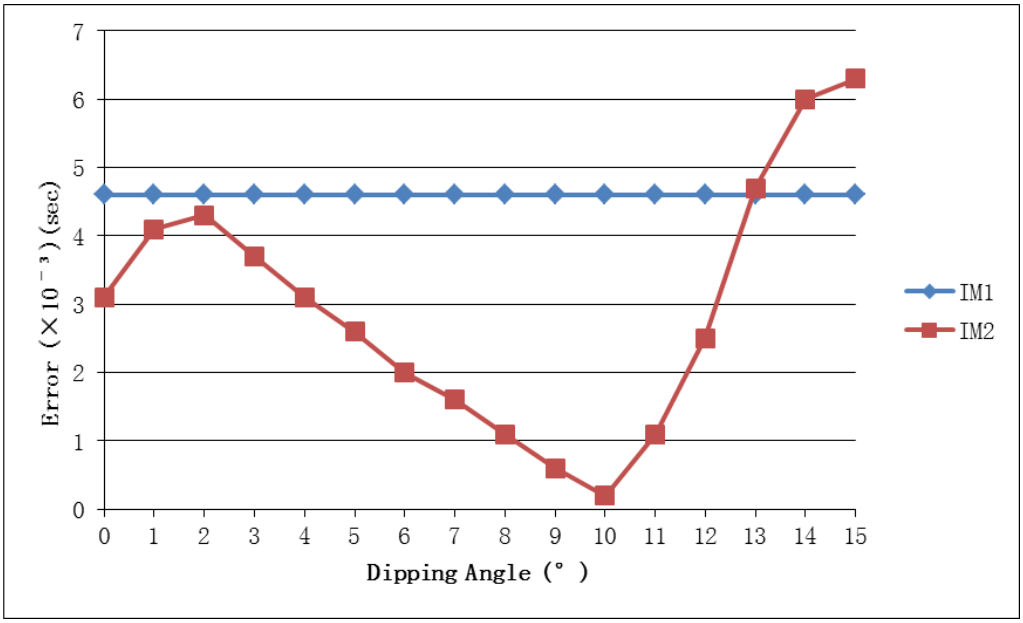

Figure 7: Prediction error in the zero offset trace plotted against an increasing series of dipping angles, the third interface is the dipping interface.

Finally, we will study the third interface, which becomes the dipping interface this time. In Figure 7, the prediction error of the first internal multiple remains constant, implying that with the increases of the dipping angle of the third interface, the position of the first internal multiple is unaffected, as is in the prediction algorithm. The general trend of the second internal multiple is such that prediction error decreases with increases in the dipping angle until 10 degrees, and sharply increases thereafter. However, all errors are within 1% for the range of 0-15 degrees, indicating a negligible influence on the algorithm for this range of dipping angles.

Towards making practical recommendations

We have numerically investigated the 1D internal multiple prediction algorithm based on the inverse scattering series in situations where the seismic physics nominally requires higher dimensional versions of the algorithm. If we set the acceptable error range at 5%, for horizontal reflectors when the offset reaches 150% of the generator depth, the resulting error becomes unacceptable in our decided sense. As for the influence of dipping angles on the prediction algorithm, we only focus on the zero offset trace, and so these results are proxies for relatively near-offset cases. When the generator becomes the dipping interface, it has the strongest effect on the algorithm. In this case, the error rises above our chosen threshold when the dipping angle exceeds 10 degrees. When the second interface is the dipping interface, a similar error measure exceeds 1% when dipping angle reaches 11 degrees. When the third interface becomes the dipping interface, the error crosses our threshold at a dipping angle beyond 15 degrees. In our studies, 10 degrees appears empirically to be.

What should be done with these results? For any particular seismic data set, given sufficient prestack data coverage, all of the prediction errors of the type we have been studying can be avoided altogether by using 1.5D, 2D, or 3D versions of the algorithm rather than the 1D version. However, the 1D version

is so fast to run, we may wish to derive as much value as we can from its use as a quick reconnoitre tool. We are moving towards a set of maximally general recommendations about when exactly this approximate use of the algorithm is appropriate, the above results represent our initial findings.

Conclusions

We employ the 1D internal multiple algorithm due to the work of Weglein and collaborators in the 1990s in MATLAB. We review the basic principles of the internal multiple prediction algorithm. Internal multiples from all possible generators are computed and shown in the output. Its performance is demonstrated using complex synthetic data sets. Some recommendations for the application of this method are given. We do not recommend applying this method when the offset reaches 150% of the generator depth. Although this theory is based on a flat layered structure, the result of small dipping angle interface is acceptable. All results up and until dipping angle equals 10 degrees show good results. Our main priority for future research is to move beyond the arbitrary choice of allowable error level. A promising avenue for achieving this goal is to quantify the error by studying the effect on adaptive subtraction of increasing travel-time shift between predicted and measured multiples.

Acknowledgements

This work was funded by the sponsors of CREWES. We thank the sponsors of CREWES for the financial support and all the staff and students in CREWES.

References

Araújo, F. V., Weglein, A. B., Carvalho, P. M., and Stolt, R. H., 1994, Inverse scattering series for multiple attenuation: an example with surface and internal multiples: SEG Expanded Abstracts, 13, 1039–1041.

Hernandez, M., and Innanen, K. A., 2012, Application of internal multiple prediction: from synthetic to lab to land data: CREWES Annual Report, 24.

Hernandez, M., Innanen, K. A., and Wong, J., 2011, Internal Multiple Attenuation based on inverse scattering: Theoretical review and implementation in synthetic data: CREWES Annual Report, 23.

Hernandez, M., Innanen, K. A., and Wong, J., 2011, Internal Multiple Attenuation based on inverse scattering: Implementation in physical model seismic data: CREWES Annual Report, 23.

Luo, Y., Kelamis, P. G., Fu, Q., Huo, S., Sindi, G., Aramco, S., Hsu, S., and Weglein, A. B., 2011, Elimination of land internal multiples based on the inverse scattering series: The Leading Edge, no. 884-889.

Weglein, A. B., Araújo, F. V., Carvalho, P. M., Stolt, R. H., Matson, K. H., Coates, R. T., Corrigan, D., Foster, D. J., Shaw, S. A., and Zhang, H., 2003, Inverse scattering series and seismic exploration: Inverse Problems , No. 19, R27–R83.

Weglein, A. B., Gasparotto, F. A., Carvalho, P. M., and Stolt, R. H., 1997, An inverse-scattering series method for attenuating multiples in seismic reflection data: Geophysics, 62, No. 6, 1975–1989.

Weglein, A. B., and Matson, K. H., 1998, Inverse scattering internal multiple attenuation: An analytic example and subevent interpretation, in SPIE Conference on Mathematical Methods in Geophysical Imaging, 108–117.

Xiao, C., Bancroft, J., Brown, J., and Cao, Z., 2003, Multiple suppression: A literature review: CREWES Annual Report, 15.